

Derivation of effective spin models from a three band model for CuO_2 -planes

E. Müller-Hartmann and A. Reischl

Institute of Theoretical Physics, University of Cologne,
Zùlpicher Str 77, D-50937 Cologne, Germany

Abstract. The derivation of effective spin models describing the low energy magnetic properties of undoped CuO_2 -planes is reinvestigated. Our study aims at a *quantitative* determination of the parameters of effective spin models from those of a multi-band model and is supposed to be relevant to the analysis of recent improved experimental data on the spin wave spectrum of La_2CuO_4 . Starting from a conventional three-band model we determine the exchange couplings for the nearest and next-nearest neighbor Heisenberg exchange as well as for 4- and 6-spin exchange terms via a direct perturbation expansion up to 12th order with respect to the copper-oxygen hopping t_{pd} . Our results demonstrate that this perturbation expansion does not converge for hopping parameters of the relevant size. Well behaved extrapolations of the couplings are derived, however, in terms of Padé approximants. In order to check the significance of these results from the direct perturbation expansion we employ the Zhang-Rice reformulation of the three band model in terms of hybridizing oxygen Wannier orbitals centered at copper ion sites. In the Wannier notation the perturbation expansion is reorganized by an exact treatment of the strong site-diagonal hybridization. The perturbation expansion with respect to the weak intersite hybridizations shows excellent convergence and the results are in agreement with the Padé approximants of the direct expansion.

Keywords: CuO_2 -planes; three-band model; Heisenberg model; four spin interactions; quantum antiferromagnets.

1 Introduction

After the discovery of the high- T_c superconducting oxides [1] it soon became clear that a minimum model for describing their electronic properties had to contain at least three bands [2] derived from the copper crystal field state $3d_{x^2-y^2}$ and from oxygen $2p_x$ and $2p_y$ orbitals [3]. In a seminal paper Zhang and Rice showed [4] that the low energy physics of the three-band model is in fact contained in an effective single-band model, the type of model which was envisaged initially by Anderson [5].

The work presented here is concerned with a reinvestigation of the derivation of effective single-band models from three-band models for CuO_2 -planes. The present paper will be confined to the study of undoped CuO_2 -planes where the effective models contain spin degrees of freedom only. Effective low energy models are derived from high energy parent models via perturbative expansions [6]. For the system of strongly correlated electrons considered here the copper-oxygen hopping t_{pd} is the expansion parameter of choice. The expansion in powers of t_{pd} is, however, not straightforward due to its rather small radius of convergence. Therefore, expansions beyond the leading order are required for obtaining reliable results. This is probably the reason why in existing derivations of the magnetic Hamiltonian of CuO_2 -planes the couplings are usually off by a factor of up to 2 [7, 8, 9]. The dominant term in the effective Hamiltonian is the Heisenberg nearest neighbor exchange obtained in fourth order which is substantially corrected by higher order contributions which we will present up to twelfth order. In eighth order ring exchange processes start to contribute four-spin terms to the effective Hamiltonian which turn out to be not at all small [10]. This is consistent with the recent interpretation of improved experimental data on the spin wave spectrum of La_2CuO_4 in terms of sizable four-spin exchange terms [11]. In comparison to these four-spin terms second and third neighbor Heisenberg terms which also first appear in eighth order turn out to be rather tiny. We have calculated all these terms up to twelfth order. It is evident from the results of these series expansions that physically relevant values of t_{pd} are larger than the radius of convergence. We find, however, that Padé approximants of these series expansions provide consistent extrapolations to the range of physically relevant model parameters.

There is an alternative approach to the perturbative treatment of three band models which shows a much better behavior of convergence and which we have also applied to obtain an independent check of the significance of

the Padé approximants derived from the direct expansion. This approach has been introduced in the paper of Zhang and Rice on the three band model in which this model was reformulated in terms of hybridizing oxygen Wannier orbitals centered at the copper ion sites [4]. In this notation the hopping Hamiltonian contains a large site-diagonal hybridization t_0 which is easily treated exactly for each copper ion site and small intersite hybridizations which are then treated safely in a perturbative fashion. Along these lines Zhang and Rice achieved not only a clever rearrangement of the t_{pd} perturbation series, but also a particularly transparent formulation of the physics of doped CuO_2 -planes in terms of “spin” and “hole” states the latter of which are known as Zhang–Rice singlets. In the effective low energy model (“ t – J model”) obtained this way neighboring “spins” experience an exchange interaction J and “holes” interchange their position with neighboring “spins” via a hopping parameter t [12]. We will show that the leading contribution to the nearest neighbor Heisenberg exchange obtained in second order in the intersite hopping is sufficient to reproduce the major features found from the direct expansion up to realistic values of t_{pd} , but is not sufficient for perfect agreement. Guided by sum rules for the hopping amplitudes in the Wannier representation we will then demonstrate how the agreement is systematically improved by including corrections of third and fourth order in the intersite hopping. The four-spin and further neighbor Heisenberg exchange terms will also be discussed in this context.

The paper is organized as follows. In the following section the three band model used in this work is briefly reviewed together with its transformation into the Wannier representation. Section III describes the principles of the perturbative derivation of effective Hamiltonians as we will use it. Section IV is devoted to the direct expansion with respect to t_{pd} and section V to the expansion in the Wannier representation. The results are summarized and conclusions are drawn in connection with the experimental evidence in section VI.

2 The three-band model

In this section we will briefly present the three-band model [2] from which our investigation is going to start and fix the notations used. For the purpose of this paper we will use a minimum three-band model with the Hamiltonian

$$H = H_\epsilon + H_U + H_{pd} \tag{1}$$

where the first term

$$H_\epsilon = \sum_{\mathbf{l}, \sigma} [\epsilon_d d_{\mathbf{l}, \sigma}^\dagger d_{\mathbf{l}, \sigma} + \epsilon_p (p_{x, \mathbf{l} + \mathbf{n}_x/2, \sigma}^\dagger p_{x, \mathbf{l} + \mathbf{n}_x/2, \sigma} + p_{y, \mathbf{l} + \mathbf{n}_y/2, \sigma}^\dagger p_{y, \mathbf{l} + \mathbf{n}_y/2, \sigma})] \quad (2)$$

describes the energies of the $3d$ - and $2p$ -orbitals involved, the second term

$$H_U = U \sum_{\mathbf{l}} d_{\mathbf{l}, \uparrow}^\dagger d_{\mathbf{l}, \uparrow} d_{\mathbf{l}, \downarrow}^\dagger d_{\mathbf{l}, \downarrow} \quad (3)$$

describes the Coulomb repulsion on the Cu^{1+} ions and the third term

$$H_{pd} = -t_{pd} \sum_{\mathbf{l}, \sigma} [d_{\mathbf{l}, \sigma}^\dagger (p_{x, \mathbf{l} + \mathbf{n}_x/2, \sigma} + p_{y, \mathbf{l} + \mathbf{n}_y/2, \sigma} - p_{x, \mathbf{l} - \mathbf{n}_x/2, \sigma} - p_{y, \mathbf{l} - \mathbf{n}_y/2, \sigma}) + h.c.]. \quad (4)$$

describes the hopping between $3d$ - and neighboring $2p$ -orbitals. Copper $3d_{x^2-y^2}$ -orbitals are placed on a square lattice in the (x, y) -plane which is spanned by unit vectors \mathbf{n}_x and \mathbf{n}_y and the vertices of which are labeled by the integer vector \mathbf{l} . Oxygen $2p_x$ - and $2p_y$ -orbitals are placed at the center of x - and y -bonds, respectively, between neighboring lattice sites.

Typical parameters for the three-band model (1) being used to model CuO_2 -planes are [13, 14]

$$\Delta_{pd} \doteq \epsilon_p - \epsilon_d = 3.6 \text{ eV}, \quad U = 8 \text{ eV}, \quad t_{pd} = 1.3 \text{ eV}. \quad (5)$$

For a direct expansion with respect to the hopping parameter t_{pd} the Hamiltonian (1) is decomposed into

$$H = H_0^p + V^p \quad \text{with} \quad H_0^p = H_\epsilon + H_U \quad \text{and} \quad V^p = H_{pd}. \quad (6)$$

Although the hopping amplitude t_{pd} is smaller than the charge transfer energy Δ_{pd} and than the Coulomb energy U it turns out that a direct expansion of the parameters of an effective low energy model with respect to t_{pd} , i.e. an expansion in powers of V^p , does not work for the parameter set (5). We will demonstrate this later explicitly and we will estimate the radius of convergence of such a direct expansion as $t_{pd}^c \approx U/16 = 0.5 \text{ eV}$. We will therefore work out this expansion to higher orders and will extract useful information from this expansion via Padé approximants.

Zhang and Rice [4] found an elegant way to reorganize the perturbation expansion by reformulating the three-band model in terms of hybridizing oxygen Wannier orbitals centered at the copper ion sites. The reformulated

model is obtained after transforming the hopping term into momentum space representation using the Fourier transformed operators

$$d_{\mathbf{l},\sigma}^\dagger = \frac{1}{\sqrt{L}} \sum_{\mathbf{k} \in BZ} e^{-i\mathbf{k}\mathbf{l}} d_{\mathbf{k},\sigma}^\dagger \quad (7)$$

and

$$p_{\alpha,\mathbf{l}+\mathbf{n}_\alpha/2,\sigma}^\dagger = \frac{1}{\sqrt{L}} \sum_{\mathbf{k} \in BZ} e^{-i\mathbf{k}(\mathbf{l}+\mathbf{n}_\alpha/2)} p_{\alpha,\mathbf{k},\sigma}^\dagger \quad (\alpha = x, y), \quad (8)$$

where L denotes the number of unit cells. With the form factor

$$f(\mathbf{k}) \doteq 2\sqrt{\sin^2 \frac{k_x}{2} + \sin^2 \frac{k_y}{2}} = 2\sqrt{1 - \frac{\cos k_x + \cos k_y}{2}} \quad (9)$$

and the normalized hybridizing Wannier orbital in momentum space representation

$$w_{\mathbf{k},\sigma} \doteq 2i(\sin \frac{k_x}{2} \cdot p_{x,\mathbf{k},\sigma} + \sin \frac{k_y}{2} \cdot p_{y,\mathbf{k},\sigma})/f(\mathbf{k}) \quad (10)$$

the hopping term reads

$$H_{pd} = -t_{pd} \sum_{\mathbf{k},\sigma} f(\mathbf{k})(d_{\mathbf{k},\sigma}^\dagger w_{\mathbf{k},\sigma} + w_{\mathbf{k},\sigma}^\dagger d_{\mathbf{k},\sigma}). \quad (11)$$

Applying the Fourier transform (7) to the Wannier operators $w_{\mathbf{k},\sigma}^\dagger$ mutually orthogonal real space Wannier orbitals $w_{\mathbf{l},\sigma}^\dagger$ centered at the copper sites are obtained. In terms of these the hopping Hamiltonian finally takes the form

$$H_{pd} = -t_{pd} \sum_{\mathbf{l},\mathbf{m},\sigma} [T_{\mathbf{l}-\mathbf{m}} d_{\mathbf{l},\sigma}^\dagger w_{\mathbf{m},\sigma} + h.c.], \quad (12)$$

where the Fourier coefficients

$$T_{\mathbf{R}} \doteq \frac{1}{L} \sum_{\mathbf{k}} f(\mathbf{k}) e^{i\mathbf{k}\mathbf{R}} = \int_{BZ} \frac{d^2\mathbf{k}}{(2\pi)^2} f(\mathbf{k}) e^{i\mathbf{k}\mathbf{R}} \quad (13)$$

of the form factor (9) have the full symmetry of the square lattice. Numerical values of these coefficients are given in Table 1.

\mathbf{R}	$T_{\mathbf{R}}$
(0, 0)	1.916183
($\pm 1, 0$), ($0, \pm 1$)	-0.280186
($\pm 1, \pm 1$)	-0.047013
($\pm 2, 0$), ($0, \pm 2$)	-0.027450
($\pm 2, \pm 1$), ($\pm 1, \pm 2$)	-0.013703

Table 1. Numerical values for $T_{\mathbf{R}}$

The coefficients $T_{\mathbf{R}}$ satisfy the sum rules

$$\begin{aligned} s_1 \doteq \sum_{\mathbf{m}} T_{\mathbf{m}} T_{1-\mathbf{m}} &= \langle f^2(\mathbf{k}) e^{i\mathbf{k}\mathbf{l}} \rangle_{\mathbf{k}} \\ &= \begin{cases} 4 & (\mathbf{l} = (0, 0)) \\ -1 & (\mathbf{l} = (\pm 1, 0) \text{ or } (0, \pm 1)) \\ 0 & (\text{else}). \end{cases} \end{aligned} \quad (14)$$

which we are going to use later. Obviously, the site-diagonal amplitude $T_{(0,0)}$ is much larger than all the other amplitudes and satisfies by itself the sum rule $s_{(0,0)} = 4$ already to 91.8%. The amplitudes to the 4 first neighbors are almost 7 times smaller than $T_{(0,0)}$ and including them the sum rule $s_{(0,0)} = 4$ is missed by only 0.35%. The amplitudes to further neighbors are much smaller again. One can show that in the limit of large distances the amplitudes drop asymptotically like

$$T_{\mathbf{R}} \sim \frac{-1}{2\pi R^3} \quad (R \rightarrow \infty). \quad (15)$$

To write the Hamiltonian (2) also in terms of Wannier states non-hybridizing $2p$ -orbitals orthogonal to the Wannier orbitals w have to be introduced. In momentum space representation they are given by

$$v_{\mathbf{k},\sigma} \doteq 2i(\sin \frac{k_y}{2} \cdot p_{x,\mathbf{k},\sigma} - \sin \frac{k_x}{2} \cdot p_{y,\mathbf{k},\sigma})/f(\mathbf{k}) \quad (16)$$

and since the $2p$ -basis sets (p_x, p_y) and (w, v) are unitarily equivalent one obtains

$$H_\epsilon = \sum_{\mathbf{l},\sigma} [\epsilon_d d_{\mathbf{l},\sigma}^\dagger d_{\mathbf{l},\sigma} + \epsilon_p (w_{\mathbf{l},\sigma}^\dagger w_{\mathbf{l},\sigma} + v_{\mathbf{l},\sigma}^\dagger v_{\mathbf{l},\sigma})]. \quad (17)$$

The Wannier representation in (12) and (17) allows a decomposition of the total Hamiltonian (1) into

$$H = H_0^w + V^w \quad (18)$$

where a major part of the hopping term (4) is incorporated in the unperturbed Hamiltonian. Using the shorthand notation

$$t_0 \doteq T_{(0,0)} t_{pd} \approx 1.916 t_{pd} \quad (19)$$

the unperturbed Hamiltonian is chosen as [4]

$$\begin{aligned} H_0^w &= \sum_{\mathbf{l}} h_{\mathbf{l}} \\ h_{\mathbf{l}} &= \sum_{\sigma} [\epsilon_d d_{\mathbf{l},\sigma}^\dagger d_{\mathbf{l},\sigma} + \epsilon_p w_{\mathbf{l},\sigma}^\dagger w_{\mathbf{l},\sigma} - t_0 (d_{\mathbf{l},\sigma}^\dagger w_{\mathbf{l},\sigma} + w_{\mathbf{l},\sigma}^\dagger d_{\mathbf{l},\sigma})] \\ &\quad + U d_{\mathbf{l},\uparrow}^\dagger d_{\mathbf{l},\uparrow} d_{\mathbf{l},\downarrow}^\dagger d_{\mathbf{l},\downarrow}. \end{aligned} \quad (20)$$

The non-hybridizing orbital v can be ignored altogether in the minimum three-band model considered here since it is always completely filled. The local Hamiltonians $h_{\mathbf{l}}$ act independently at each site \mathbf{l} . They are easily diagonalized exactly. The perturbative part of the total Hamiltonian is then given by the intersite hopping terms in Wannier representation

$$V^w = -t_{pd} \sum_{\mathbf{l}, \mathbf{m}, \sigma}^{\mathbf{l} \neq \mathbf{m}} T_{\mathbf{l}-\mathbf{m}} [d_{\mathbf{l}, \sigma}^\dagger w_{\mathbf{m}, \sigma} + w_{\mathbf{l}, \sigma}^\dagger d_{\mathbf{m}, \sigma}] \quad (21)$$

which are so small that they can safely be treated perturbatively for model parameters as given by (5). The separation of energy scales between H_0^w and V^w achieved through the use of the Wannier representation is so substantial that it is hard to understand why a controversy about the scenario proposed by Zhang and Rice [4] arose early on [15, 16, 17, 18, 19] which was still quoted as unsettled in the review by Dagotto [12]. Leading order perturbative calculations using the Wannier representation were performed by many authors (see, e.g., [20, 21, 22]).

3 Perturbative derivation of effective Hamiltonians

The perturbative derivation of effective Hamiltonians for correlated electron systems has a long history the early stages of which were summarized by Takahashi in 1977 [6]. In this paper Takahashi presents a particularly transparent description of the method and gives an explicit solution for the effective Hamiltonian to arbitrary order. We will briefly recall Takahashi's approach here, because we are going to perform the perturbation expansions in this paper using his formulation and because we wish to avoid controversies about the proper use of the method like in [23, 24].

It is assumed that the total Hamiltonian of a system is decomposed into

$$H = H_0 + V. \quad (22)$$

In the case of interest H_0 has a degenerate subspace U_0 of ground states with energy E_0 . On switching on the perturbation V continuously the subspace U_0 evolves continuously into the subspace U of the corresponding low energy eigenspace of H . Takahashi presents an explicit perturbative formula to all

orders in V for an isometric linear transformation $\Gamma: U_0 \rightarrow U$ describing the mapping of U_0 onto U . In terms of Γ the effective Hamiltonian is then given by

$$H_{\text{eff}} = \Gamma^\dagger H \Gamma. \quad (23)$$

It acts in the subspace U_0 of unperturbed eigenstates of H_0 and has the same spectrum as the perturbed Hamiltonian H . In view of the explicit perturbation series of Γ it is a pure problem of book-keeping to set up the perturbation series for H_{eff} to any required order. In terms of the projection operator P_0 onto the ground state subspace U_0 and the resolvent operator

$$S \doteq -\frac{1 - P_0}{H_0 - E_0} \quad (24)$$

the full perturbation expansion up to fourth order is given by

$$\begin{aligned} H_{\text{eff}} = & E_0 P_0 + P_0 V P_0 + P_0 V S V P_0 \\ & + P_0 V S V S V P_0 - \frac{1}{2} P_0 V P_0 V S^2 V P_0 - \frac{1}{2} P_0 V S^2 V P_0 V P_0 \\ & + P_0 V S V S V S V P_0 - \frac{1}{2} P_0 V S^2 V P_0 V S V P_0 - \frac{1}{2} P_0 V S V P_0 V S^2 V P_0 \\ & + \frac{1}{2} P_0 V P_0 V P_0 V S^3 V P_0 + \frac{1}{2} P_0 V S^3 V P_0 V P_0 V P_0 \\ & - \frac{1}{2} P_0 V P_0 V S^2 V S V P_0 - \frac{1}{2} P_0 V S V S^2 V P_0 V P_0 \\ & - \frac{1}{2} P_0 V P_0 V S V S^2 V P_0 - \frac{1}{2} P_0 V S^2 V S V P_0 V P_0. \end{aligned} \quad (25)$$

For the purposes of the calculations in this paper we had to list this expansion up to twelfth order. The number of terms in the series grows exponentially with the order. To twelfth order the perturbation series contains 363721 terms.

For useful applications of the formal series of H_{eff} the unperturbed Hamiltonian H_0 has to be easily diagonalized such that matrix elements of the resolvent (24) can be calculated explicitly. In this paper we will apply the perturbation expansion to the two Hamiltonian decompositions (6) and (18) where this condition on H_0 is satisfied. We also will confine the analysis to undoped systems which implies that all terms in H_{eff} containing $P_0 V P_0$ don't contribute. This reduces the number of twelfth order terms in H_{eff} to 12341. In the direct expansion based on (6) ground states can only be connected

by an even number of hopping processes such that all terms with any odd number of V between two P_0 don't contribute. This reduces the number of twelfth order terms to 3180. For the Wannier decomposition (18) our analysis will be confined to sixth order. In this case, of the terms given in (25) only the second order term, the first third order term and the first three fourth order terms will contribute and up to sixth order 30 terms have to be taken into account. Notice that in the Wannier decomposition (18) odd order terms do contribute since H_0^w mixes d- and w-orbitals.

4 Direct perturbation expansion

In this section we are going to discuss the direct expansion with respect to t_{pd} on the basis of the decomposition (6). In the undoped case that we are considering here the subspace of ground states U_0 of the unperturbed Hamiltonian H_0^p contains all states with completely filled p-orbitals and with a single d-hole on each copper site. The effective Hamiltonian acting on U_0 is thus a pure spin Hamiltonian acting on the spins $S = 1/2$ of the d-sites. Due to the symmetry properties of the three band model (1) this Hamiltonian has got to be invariant under global spin rotations and under the space group of the square lattice. Only terms with an even number of spins are possible due to time reversal symmetry. The excited states of H_0^p are very simple and the excitation energies contain a Coulomb energy U for each doubly occupied d-site and a charge transfer energy $-\Delta_{pd}$ for each p-hole. For a contribution of order n to the effective Hamiltonian one has to consider all sets of n hopping processes each of which defines a certain cluster of sites involved. Due to the linked cluster theorem (which is bound to hold to keep the effective Hamiltonian extensive) only connected clusters are known to contribute. It is therefore sufficient to evaluate the various orders of H_{eff} on certain finite clusters. We have implemented the purely symbolic evaluation of the series expansion with a C++ program.

For simplicity we will disregard any constant energy shift in H_{eff} since we want to focus on the effective spin Hamiltonian. The leading term in H_{eff} is then a fourth order nearest neighbor Heisenberg exchange $J_1 \mathbf{S}_1 \cdot \mathbf{S}_2$ with the well known exchange coupling [25]

$$J_{1,\text{dir}}^{(4)} = \frac{2t_{pd}^4}{(U - \Delta_{pd})^2} \left(\frac{4}{2(U - \Delta_{pd})} + \frac{2}{U} \right) = \frac{4t_{pd}^4(2U - \Delta_{pd})}{U(U - \Delta_{pd})^3}. \quad (26)$$

In order to determine this coupling it is sufficient to calculate the amplitude of a spin flip process on a three-site cluster consisting of two neighboring d-sites and the p-site in between. In view of the identity $\mathbf{S}_1 \cdot \mathbf{S}_2 = S_1^z S_2^z + \frac{1}{2}(S_1^+ S_2^- + S_1^- S_2^+)$ the coupling is given by twice the spin flip amplitude.

In sixth order processes the six additional p-sites adjacent to the two d-sites can be visited by a hole. Therefore a nine site cluster would be sufficient to calculate $J_{1,\text{dir}}^{(6)}$. Since in each individual exchange process at most one of the additional p-sites is visited the actual calculation can be confined to clusters of up to no more than four sites. Each of the six four-site clusters gives the same contribution to the sixth order coupling. In one such contribution either all four sites or only the three sites of the fourth order cluster will be involved in the exchange process. Therefore, the sixth order spin flip amplitude is given by six times the spin flip amplitude of the four-site cluster minus 5 times the spin flip amplitude of the three-site cluster. This type of reasoning would be dispensable in the sixth order case for which it was exemplified here, but it is absolutely essential to make the higher order calculations feasible. It allows to reduce the maximum cluster size for the calculation of the nearest neighbor exchange from 17 to 8 in eighth order, from 31 to 9 in tenth order and from 43 to 12 in twelfth order.

In eighth order ring exchange processes on an eight-site plaquette visiting four d-sites are possible. These processes produce four-spin exchange terms in H_{eff} . In cases where multi-spin terms are present the fewer-spin exchange terms can be inferred in the following way. Partial traces (i.e. traces over some of the spins) of any multi-spin term vanish. By forming the trace over some of the spins belonging to a cluster all exchange terms containing these spins are therefore projected out. Applying this reasoning to the eight-site plaquette one obtains the two-spin exchange of a pair of spins by averaging over all configurations of the other spins contained in the plaquette. From time reversal invariance and hermiticity of H_{eff} one can infer that the amplitude of a spin flip process remains unchanged if all unflipped spins of a cluster are inverted. This allows to reduce by a factor of 2 the number of configurations needed for the averaging.

Along the lines described above we have calculated the nearest neighbor exchange coupling $J_{1,\text{dir}}$ up to twelfth order in t_{pd} . The full formula of the twelfth order result is given by Eq. (A.1) in Appendix A. Fig. 1 shows how the ratio $J_{1,\text{dir}}/J_{1,\text{dir}}^{(4)}$ varies with increasing t_{pd} if the sixth, eighth, tenth and twelfth order terms are included (see the thick lines in Fig. 1). It is

obvious from this plot that for the physically relevant values of t_{pd} as given

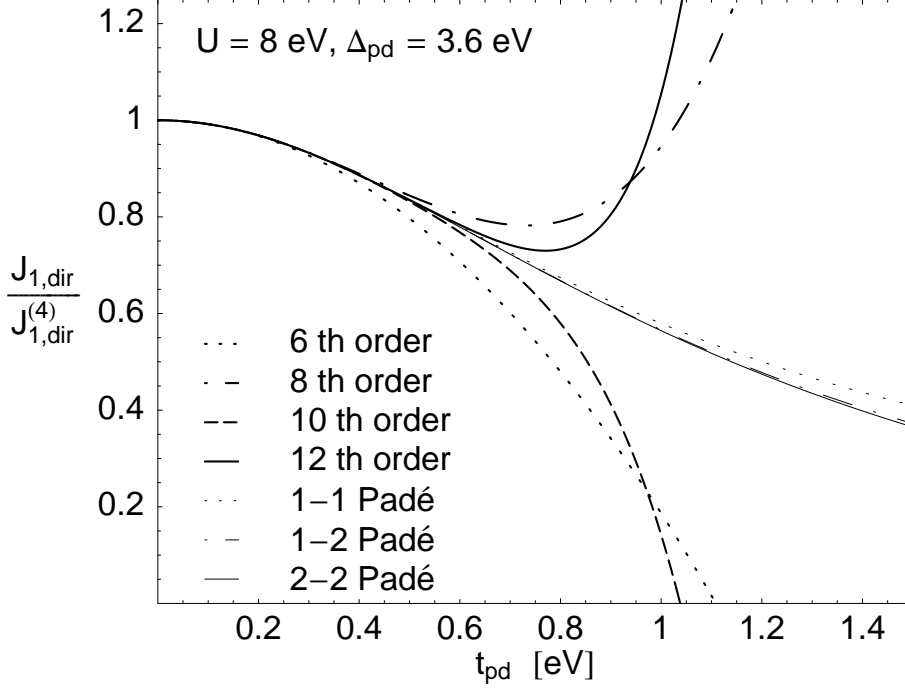


Figure 1: Variation of $J_{1,\text{dir}}/J_{1,\text{dir}}^{(4)}$ with t_{pd} .

in (5) J_1 is smaller than simple estimates from $J_{1,\text{dir}}^{(4)}$ would suggest, but it is also obvious that the radius of convergence of the direct perturbation series considered here is much smaller than $t_{pd} = 1.3 \text{ eV}$. The direct series determines J_1 accurately only up to $t_{pd} \approx 0.5 \text{ eV}$. Extrapolations beyond the radius of convergence can be obtained, however, via Padé approximants of the series for $J_{1,\text{dir}}/J_{1,\text{dir}}^{(4)}$. We denote as m-n Padé the approximant with an m^{th} order numerator polynomial and an n^{th} order denominator polynomial in the variable $x = t_{pd}^2$. We have also constructed extrapolations via analogous Padé approximants for the logarithmic derivative of $J_{1,\text{dir}}/J_{1,\text{dir}}^{(4)}$ which we denote by m-n DlogPadé. The 1-1, 1-2 and 2-2 Padés shown by the thin lines in Fig. 1 demonstrate the excellent convergence of this extrapolation procedure. The 1-3 Padé and the 1-2 and 0-2 DlogPadés are not shown because they all differ from the 2-2 Padé by less than 0.4% for $t_{pd} \leq 1.5 \text{ eV}$. From this observation

we derive the conservative estimate that they determine the nearest neighbor exchange coupling with an accuracy of better than 1%. Note the substantial reduction of the coupling in the range of physical interest, $J_1 = 0.44 J_{1,\text{dir}}^{(4)}$ for $t_{pd} = 1.3 \text{ eV}$, in comparison to the lowest order result.

The four-spin exchange terms which first appear in eighth order can be inferred from considering processes in which all four spins are flipped. Let us label the spins on the four d-sites of a square plaquette in cyclic order by numbers 1 to 4. There are 3 independent four-spin invariants, $(\mathbf{S}_1 \cdot \mathbf{S}_2)(\mathbf{S}_3 \cdot \mathbf{S}_4)$, $(\mathbf{S}_2 \cdot \mathbf{S}_3)(\mathbf{S}_4 \cdot \mathbf{S}_1)$ and $(\mathbf{S}_1 \cdot \mathbf{S}_3)(\mathbf{S}_2 \cdot \mathbf{S}_4)$ from which the four-spin exchange terms have to be formed. Due to the square point symmetry of our model the first two invariants always get the same exchange coupling in the effective Hamiltonian. This common coupling is given by twice the amplitude of the process which flips all spins of the initial state $|1 \uparrow, 2 \downarrow, 3 \uparrow, 4 \downarrow\rangle$, since the third invariant doesn't contribute to this process. The exchange coupling of the third invariant can be inferred from considering an alternative four-spin flip process starting from the initial state $|1 \uparrow, 2 \downarrow, 3 \downarrow, 4 \uparrow\rangle$. The sum of the couplings of the first invariant and the third invariant is given by four times the amplitude of this process. It turns out that this amplitude vanishes in eighth and tenth order. This implies that up to tenth order the four-spin exchange term has the form

$$J_{\square} \left[(\mathbf{S}_1 \cdot \mathbf{S}_2)(\mathbf{S}_3 \cdot \mathbf{S}_4) + (\mathbf{S}_2 \cdot \mathbf{S}_3)(\mathbf{S}_4 \cdot \mathbf{S}_1) - (\mathbf{S}_1 \cdot \mathbf{S}_3)(\mathbf{S}_2 \cdot \mathbf{S}_4) \right] \quad (27)$$

in analogy to what is known for the one band Hubbard model in fourth order [6].

The vanishing of the $|1 \uparrow, 2 \downarrow, 3 \downarrow, 4 \uparrow\rangle$ spin flip process up to tenth order can be easily understood as resulting from the linked cluster theorem, because for these processes the plaquette (1,2,3,4) decomposes into two unlinked clusters, one of them containing the d-sites 1 and 2, the other containing sites 3 and 4. In twelfth order there are processes linking these two clusters and producing another four-spin term

$$J_{\times} (\mathbf{S}_1 \cdot \mathbf{S}_3)(\mathbf{S}_2 \cdot \mathbf{S}_4) \quad (28)$$

in addition to (27). It has to be noted that in twelfth order clusters containing 6 d-sites are created which produce six-spin terms in the effective Hamiltonian. In the calculation of the four-spin terms these six-spin terms have to be properly eliminated by the averaging procedure described above.

The eighth order coupling constant of the four-spin term (27) is found to

be

$$J_{\square,\text{dir}}^{(8)} = \frac{80 t_{pd}^8 (2U - \Delta_{pd})(3U^2 - 3U\Delta_{pd} + \Delta_{pd}^2)}{U^3(U - \Delta_{pd})^7}. \quad (29)$$

Corrections up to fourteenth order are shown by Eq. (A.2) in Appendix A together with the leading order contribution for J_{\times} in Eq. (A.3). The variation of $J_{\square,\text{dir}}/J_{\square,\text{dir}}^{(8)}$ with increasing t_{pd} is shown in Fig. 2. Here, the 2-1 Padé (not shown) and the 1-1 and the 0-2 Padés as well as the 0-2 DlogPadé seem to provide a rather accurate estimate with an uncertainty of about $\pm 3\%$ for $t_{pd} = 1.3$ eV and an uncertainty of about $\pm 7\%$ for $t_{pd} = 1.5$ eV. For $t_{pd} = 1.3$ eV the coupling J_{\square} is about 5 times smaller than suggested by the leading order term. We will consider the 0-2 DlogPadé the most probable estimate of $J_{\square,\text{dir}}/J_{\square,\text{dir}}^{(8)}$.

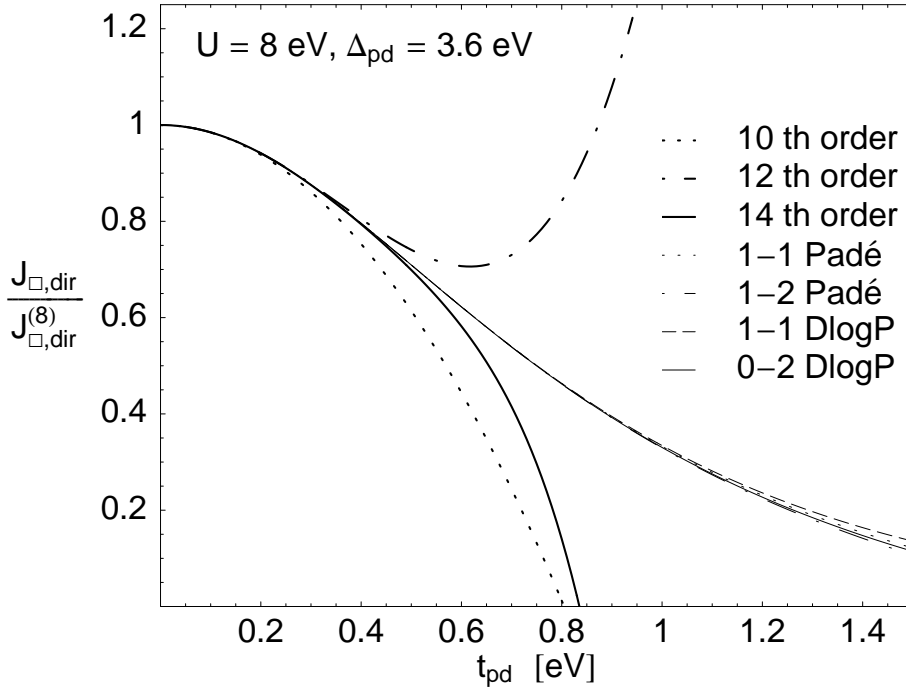


Figure 2: Variation of $J_{\square,\text{dir}}/J_{\square,\text{dir}}^{(8)}$ with t_{pd} .

The leading contributions to second neighbor Heisenberg exchange terms like $J_2 \mathbf{S}_{(0,0)} \cdot \mathbf{S}_{(1,1)}$ and to third neighbor Heisenberg exchange terms like

$J_3 \mathbf{S}_{(0,0)} \cdot \mathbf{S}_{(0,2)}$ are also obtained in eighth order. These couplings are given by

$$J_{2,\text{dir}}^{(8)} = \frac{4 t_{pd}^8 (18 U^3 - 11 U^2 \Delta_{pd} + 5 U \Delta_{pd}^2 - \Delta_{pd}^3)}{U^3 (U - \Delta_{pd})^7} \quad (30)$$

and

$$J_{3,\text{dir}}^{(8)} = \frac{4 t_{pd}^8 (8 U^3 - 9 U^2 \Delta_{pd} + 5 U \Delta_{pd}^2 - \Delta_{pd}^3)}{U^3 (U - \Delta_{pd})^7}, \quad (31)$$

respectively. Corrections to these leading order expressions which we have calculated to twelfth order are given by Eqs. (A.4) and (A.5) in Appendix A.

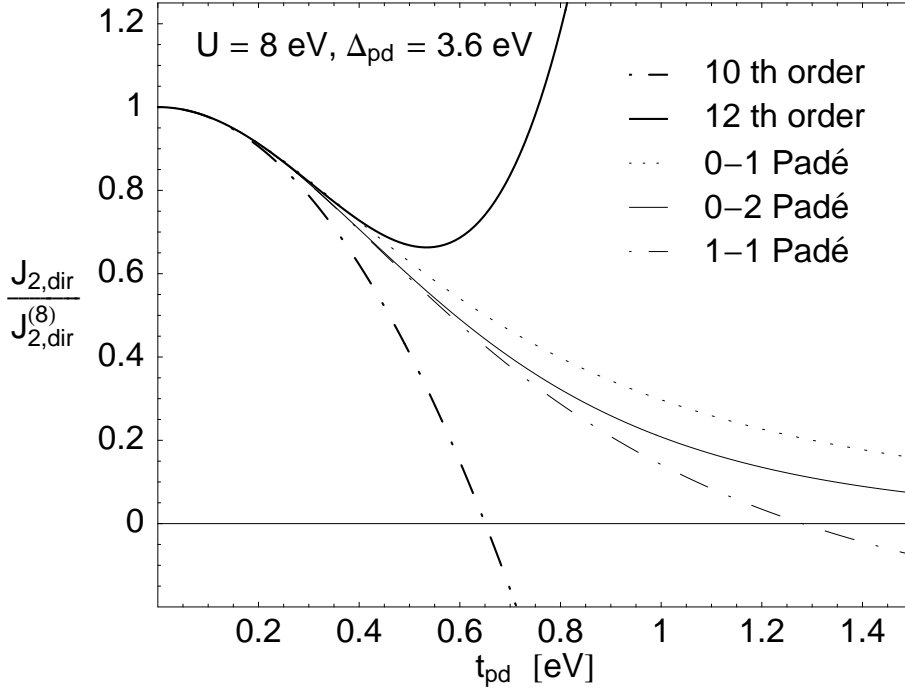


Figure 3: Variation of $J_{2,\text{dir}}/J_{2,\text{dir}}^{(8)}$ with t_{pd} .

Figs. 3 and 4 show the variation of $J_{2,\text{dir}}/J_{2,\text{dir}}^{(8)}$ and $J_{3,\text{dir}}/J_{3,\text{dir}}^{(8)}$, respectively, with increasing t_{pd} . The radii of convergence appear to be even smaller than in the case of J_1 . The 1-1 Padé in Fig. 3 might indicate that J_2 changes

sign slightly below $t_{pd} = 1.3$ eV, but the scattering of the various approximants doesn't allow definite conclusions on a change of sign. Since the 0-1 DlogPadé (not shown in Fig. 3) coincides to high precision with the 0-2 Padé we will consider this approximant as the most probable estimate for J_2 . The 0-2 Padé for J_3 shown in Fig. 4 turns upwards and has a pole at $t_{pd} \approx 2$ eV. The other three approximants shown appear to behave consistently and we will consider the 0-1 DlogPadé as the most probable estimate for J_3 . Altogether, the Padé approximants for J_2 and J_3 scatter much more than those for J_1 and J_\square and provide less accurate estimates for J_2 and J_3 . We do, however, learn from these extrapolations that for $t_{pd} = 1.3$ eV both J_2 and J_3 also are reduced substantially in comparison to the leading order results (30) and (31), J_2 probably by a factor of a much as 10 and J_3 probably by a factor of 4. As we will see later J_2 and J_3 are so small in absolute size that their accurate determination is less urgent for practical purposes.

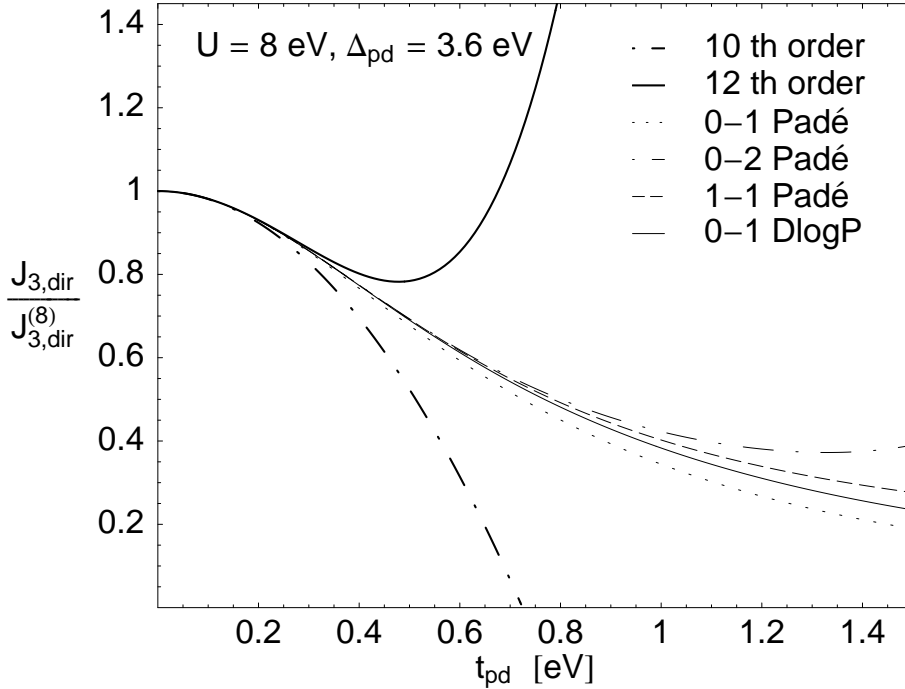


Figure 4: Variation of $J_{3,dir}/J_{3,dir}^{(8)}$ with t_{pd} .

To describe the six-spin term resulting from twelfth order ring exchange processes on a double plaquette we label the six spins involved cyclically by numbers 1 to 6. Since the oxygen ion at the center of the double plaquette is not visited in twelfth order the six-spin term has the full symmetry of the hexagon formed by the six spins. The 15 independent invariants obtained by all pairings of the six spins into three scalar products [26] group into the 5 operators with hexagonal symmetry O_1 to O_5 given by Eq. (A.6) in Appendix A. With the same type of arguments which led to (27) we conclude that the twelfth (and fourteenth) order six-spin term has the form

$$J_{\square}(O_1 + O_2 - O_3 + O_4 - O_5). \quad (32)$$

The exchange coupling $J_{\square}^{(12)}$ given by Eq. (A.7) in Appendix A was calculated from ring exchange processes which flip all spins of the state $|1\uparrow, 2\downarrow, 3\uparrow, 4\downarrow, 5\uparrow, 6\downarrow\rangle$. For a comparison of the relative sizes of the various cou-

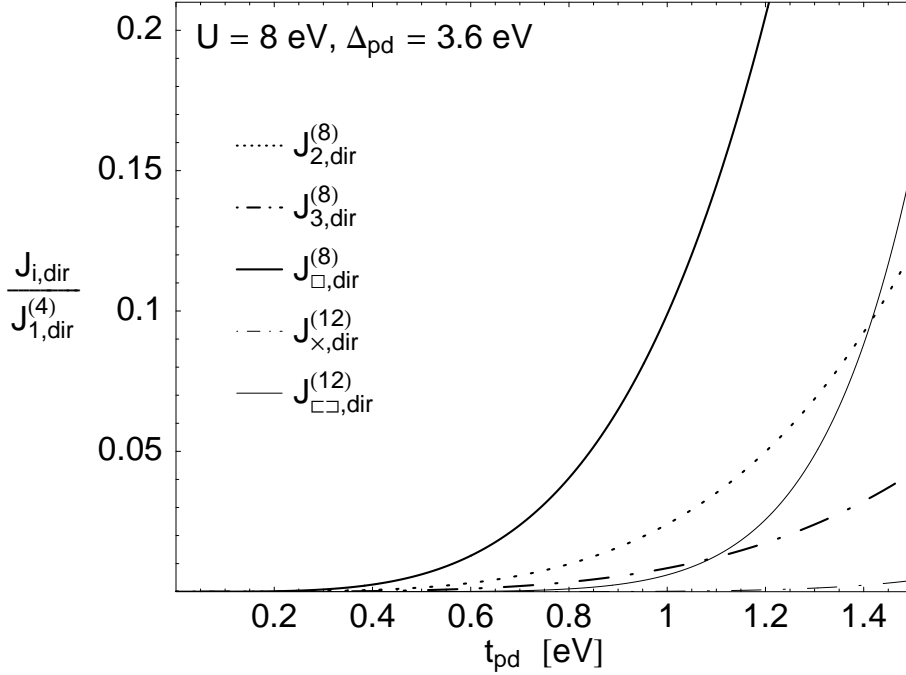


Figure 5: Comparison of the leading order terms of the various couplings.

plings we first show in Fig. 5 the leading perturbative contributions of all

couplings determined, in units of $J_{1,\text{dir}}^{(4)}$. In the range of physically relevant model parameters the four-spin coupling J_{\square} is by far the largest correction to the nearest neighbor two-spin coupling J_1 . The second and third neighbor Heisenberg couplings J_2 and J_3 are much smaller and are in fact comparable to the six-spin coupling J_{\square} . This scenario agrees with what is known from perturbation expansions for the single band Hubbard model [6, 24] and from cluster calculations for the three band model [10].

A quantitative comparison of the best approximants for the various couplings with J_1 (represented by its 2-2 Padé) is shown in Fig. 6 where we have denoted the m-n Padé for the coupling J_i by $J_i[m, n]$. For the model parameters (5), J_{\square} is about one order of magnitude smaller than J_1 and the couplings J_2 and J_3 are about another order of magnitude smaller. The four-spin coupling J_{\square} therefore has to be considered an important modification of the simple nearest neighbor Heisenberg model, whereas the second and third neighbor Heisenberg couplings J_2 and J_3 (as well as the six-spin coupling J_{\square}) may be ignored as correction at the level of about 2%.

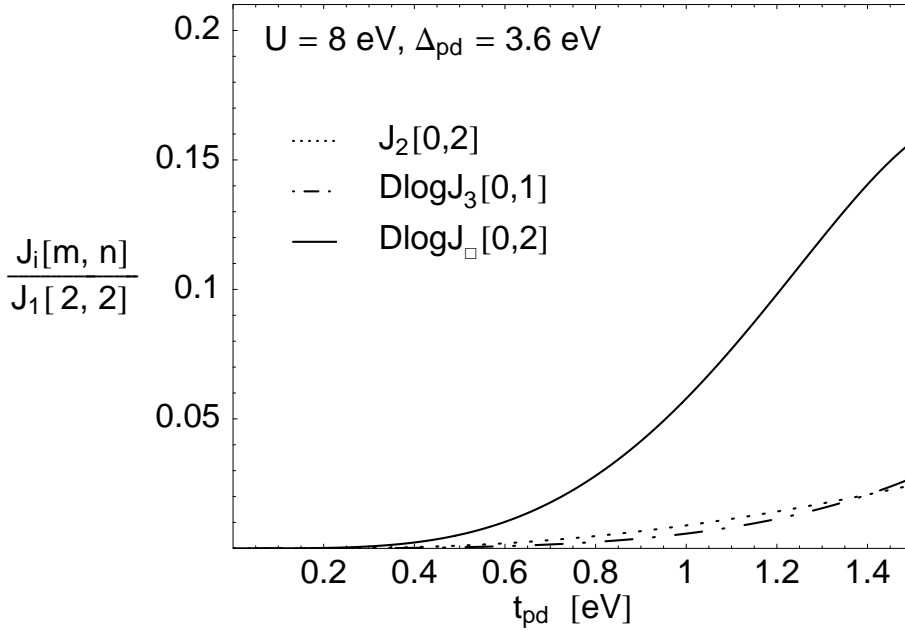


Figure 6: Comparison of the best Padé approximants.

5 Expansion in the Wannier representation

In this section we are going to discuss an alternative perturbation expansion based on the decomposition (18) of the three band Hamiltonian. The unperturbed Hamiltonian (20) consists of independent local Hamiltonians h_1 for each site which are easily diagonalized. In the one hole sector the local Hamiltonian has two $S = 1/2$ eigenstates where mutually orthogonal linear combinations of d-hole and w-hole orbitals are occupied. The two hole sector contains a non-hybridized $S = 1$ triplet and three hybridized singlets the lowest one of which is the Zhang-Rice singlet. In the three hole sector again two $S = 1/2$ doublets are found. The four hole sector and the zero hole sector each contain one trivial $S = 0$ state. The lower doublet in the one hole sector acts as the local ground state doublet of the undoped system. All the other states will show up as intermediate excited states at sufficiently high orders of the expansion with respect to the perturbation (21). We have diagonalized the local Hamiltonian numerically. A simple analytic formula cannot be obtained in the general case since for the three singlets in the two hole sector a (3×3) -matrix has to be diagonalized. Simple analytic expressions for the solution in this sector would be available only in the symmetric case $\Delta_{pd} = U/2$. The perturbation expansion with respect to (21) was performed using a combination of symbolic and numerical routines.

It is instructive to analyse the radius of convergence t_{pd}^c of the local Hamiltonian h_1 which does depend on t_{pd} via (19). This radius of convergence can be determined from studying the branch points of the eigenvalues of the local Hamiltonian in the complex t_{pd} -plane. Without going into any details we wish to summarize this analysis here by stating that $t_{pd}^c = 0.469 \text{ eV}$ for the values of U and Δ_{pd} given in (5). This value agrees well with the values estimated from the Padé approximants. This is not surprising since the expansion with respect to the small perturbation (21) is expected to converge well and should not much modify t_{pd}^c as defined above from the local Hamiltonian.

In what follows we will plot the variation of the various coupling constants with the hopping t_{pd} in analogy to the presentations in the previous figures by measuring all couplings in units of their lowest order term in the direct expansion (if not otherwise stated). Fig. 7 shows our results for the nearest neighbor exchange $J_{1,w}$. In the present context the leading contribution to $J_{1,w}$ is obtained from the simple second order hopping process described by the term $P_0 V S V P_0$ of (25). This second order contribution is depicted by

the thick dotted line in Fig. 7. It is satisfying that this simple second order result reproduces quite nicely the decrease of $J_1/J_{1,\text{dir}}^{(4)}$ with increasing t_{pd} as given by the Padé approximants of Fig. 1. On the other hand, there is, however, a systematic deviation in the overall size of the coupling; even for small t_{pd} the coupling $J_{1,w}^{(2)}$ is too large by about 15%. The discrepancy at small t_{pd} is largely reduced by taking into account the third order terms derived from P_0VSVSP_0 and, finally, $J_{1,w}^{(4)}$ is in perfect agreement with the 2-2 Padé of the direct expansion. The deviation of $J_{1,w}^{(2)}$ from $J_{1,\text{dir}}^{(4)}$ for small

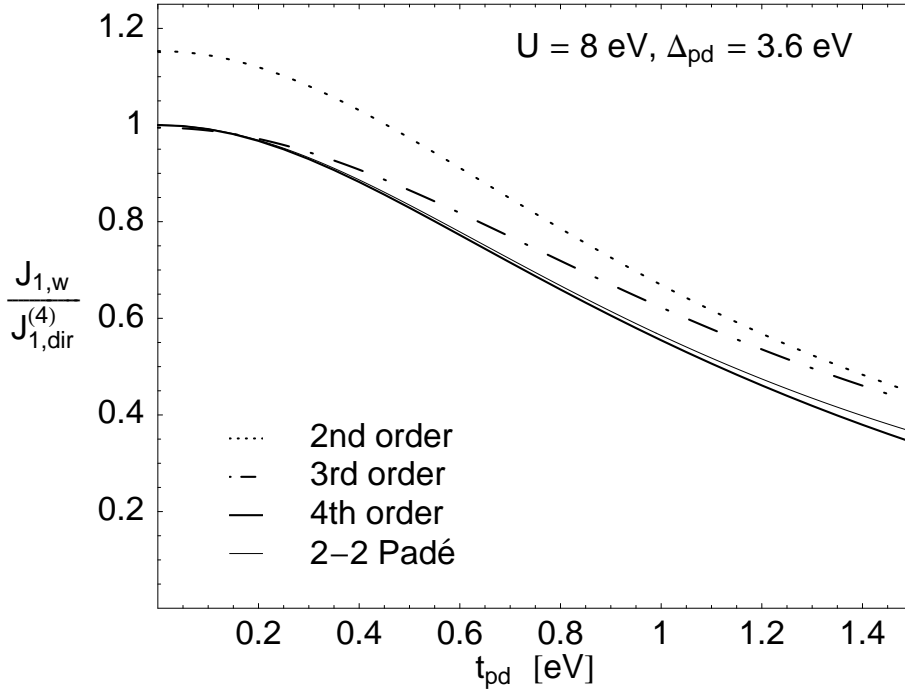


Figure 7: Variation of $J_{1,w}/J_{1,\text{dir}}^{(4)}$ with t_{pd} .

t_{pd} is explained quantitatively by re-expanding $J_{1,w}^{(2)}$ to second order with respect to t_0 . Referring to (19) we obtain

$$J_{1,w}^{(2)} \sim (2T_{(0,0)}T_{(1,0)})^2 J_{1,\text{dir}}^{(4)} \quad (t_{pd} \rightarrow 0) \quad (33)$$

which explains the 15% deviation because $(2T_{(0,0)}T_{(1,0)})^2 = 1.153$. Since $J_{1,w}^{(4)}$ collects all fourth order terms it has to coincide with $J_{1,\text{dir}}^{(4)}$ after re-expanding

it to t_{pd}^4 . How this happens becomes particularly clear if one looks at the sum rule $s_{(1,0)}$ of (14). This sum rule states that $2T_{(0,0)}T_{(1,0)} + r_{(1,0)} = -1$ if we denote by $r_{(1,0)}$ the sum of all terms in $s_{(1,0)}$ (infinitely many) which don't contain $T_{(0,0)}$. Squaring this sum rule we obtain the relation

$$(2T_{(0,0)}T_{(1,0)})^2 + 2(2T_{(0,0)}T_{(1,0)})r_{(1,0)} + r_{(1,0)}^2 = 1 \quad (34)$$

from which we can read off the contributions of various orders of the Wannier expansion to $J_{1,\text{dir}}^{(4)}$ in the limit of small t_{pd} . The first term represents the contribution of $J_{1,w}^{(2)}$ discussed above. The second term contains only one factor of $T_{(0,0)}$ and results from third order terms in V^w which due to $r_{(1,0)} = 0.073775$ exhaust the relation (34) to $1 - r_{(1,0)}^2 = 0.994557$; this explains why $J_{1,w}^{(3)}$ is slightly smaller than $J_{1,\text{dir}}^{(4)}$ in the limit of small t_{pd} (see Fig. 7). Finally, the term $r_{(1,0)}^2$ comes from fourth order terms in V^w which contribute only about 0.5% for small t_{pd} but change sign and get more important as t_{pd} increases.

In our calculation of third and fourth order contributions to $J_{1,w}$ we have made extensive use of the sum rule $s_{(1,0)}$. In third order terms the exchange path for a spin flip process involves an arbitrary third copper ion site whose spin is not flipped. The sum of the spin flip amplitudes over all these third sites contains a lattice sum which is simply $r_{(1,0)}$. The calculation of the fourth order is more involved since one has to discriminate between spin flip processes which don't visit another site and those which visit one or two more sites. The lattice sums appearing in this order cannot be completely determined from sum rules, but sum rules considerably simplify their calculation. Four-spin terms which here appear in fourth order are eliminated by averaging as described in the previous section.

Results for the four-spin coupling $J_{\square,w}$ are shown in Fig. 8. The leading fourth order contribution again nicely reproduces qualitatively the decrease with increasing t_{pd} known from Fig. 2. After the above discussion the deviation observed in the small t_{pd} limit is not surprising. In fact, a quantitative understanding of this deviation follows from looking at the fourth power of the $s_{(1,0)}$ sum rule: $(2T_{(0,0)}T_{(1,0)} + r_{(1,0)})^4 = 1$. With $(2T_{(0,0)}T_{(1,0)})^4 = 1.329$ we understand why $J_{\square,w}^{(4)}$ is about 33% too large for small t_{pd} . The substantial reduction of the deviation by the fifth order contributions are also understood quantitatively from the identity $(2T_{(0,0)}T_{(1,0)})^4 + 4(2T_{(0,0)}T_{(1,0)})^3r_{(1,0)} = 0.964$ (see Fig. 8). Including the sixth order terms we find the almost negligible deviation of $(2T_{(0,0)}T_{(1,0)})^4 + 4(2T_{(0,0)}T_{(1,0)})^3r_{(1,0)} + 6(2T_{(0,0)}T_{(1,0)})^2r_{(1,0)}^2 = 1.0017$

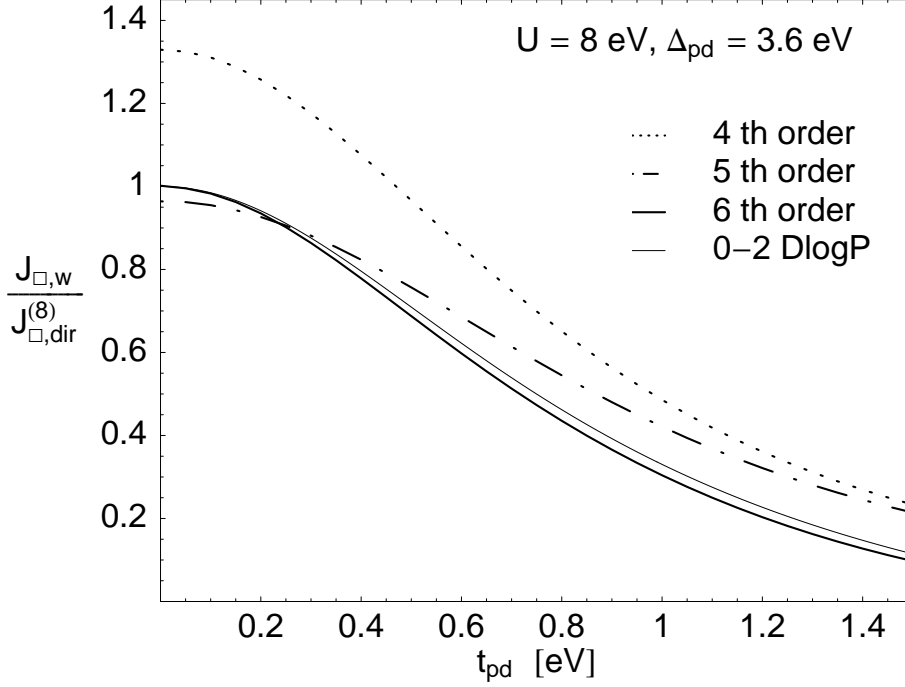


Figure 8: Variation of $J_{\square,w}/J_{\square,\text{dir}}^{(8)}$ with t_{pd} .

and the overall agreement with the 0-2 DlogPadé is quite satisfying.

The analysis of the second and third neighbor exchange J_2 and J_3 is more complicated in the Wannier representation since there are low order contributions which have to be cancelled completely by higher order terms before results of any significance emerge. We therefore show these couplings in Figs. 9 and 10 not in units of their eighth order counterparts from the direct expansion but in units of $J_{1,\text{dir}}^{(4)}$. It is quite obvious that for any lattice vector \mathbf{l} there is a second order contribution $J_{1,w}^{(2)}$ to the Heisenberg coupling between two spins separated by \mathbf{l} which in analogy to (33) behaves like

$$J_{1,w}^{(2)} \sim (2T_{(0,0)}T_1)^2 J_{1,\text{dir}}^{(4)} \quad (t_{pd} \rightarrow 0). \quad (35)$$

The cancellation of this contribution by higher order terms is understood by invoking the sum rule $2T_{(0,0)}T_1 + r_1 = 0$ for further neighbors which squared

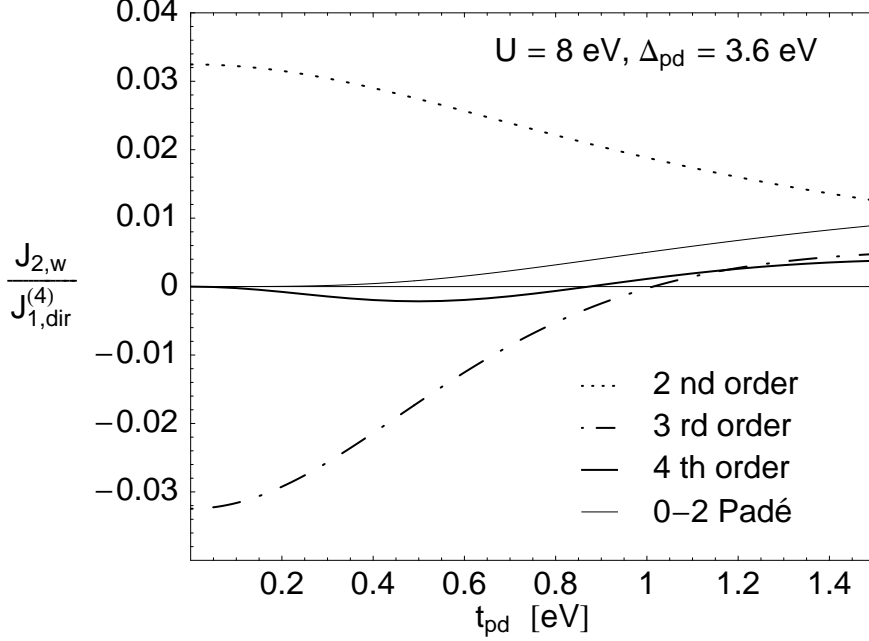


Figure 9: Variation of $J_{2,w}/J_{1,dir}^{(4)}$ with t_{pd} .

gives the relation

$$(2T_{(0,0)}T_1)^2 + 2(2T_{(0,0)}T_1)r_1 + r_1^2 = 0. \quad (36)$$

The numbers $(2T_{(0,0)}T_{(1,1)})^2 = 0.0325$ and $(2T_{(0,0)}T_{(2,0)})^2 = 0.0111$ coincide perfectly with the behavior of $J_{2,w}^{(2)}$ and $J_{3,w}^{(2)}$ for small t_{pd} as shown in Figs. 9 and 10. We also understand from (36) why the inclusion of the third order doesn't reduce the deviation from 0 but just changes its sign. In fourth order Fig. 9 shows that in agreement with (36) the terms proportional to t_{pd}^4 in $J_{2,w}$ vanish. This is, however, only a partial solution of the cancellation problem since there are still terms proportional to t_{pd}^6 which according to Fig. 9 even have the wrong sign and cancellation of which would only be achieved by extending the V^w expansion to sixth order. For $t_{pd} > 1$ eV the third and fourth order results shown in Figs. 9 and 10 at least have the right sign and the same order of magnitude as the Padé estimates from the previous section. We have to conclude that the accurate determination of the

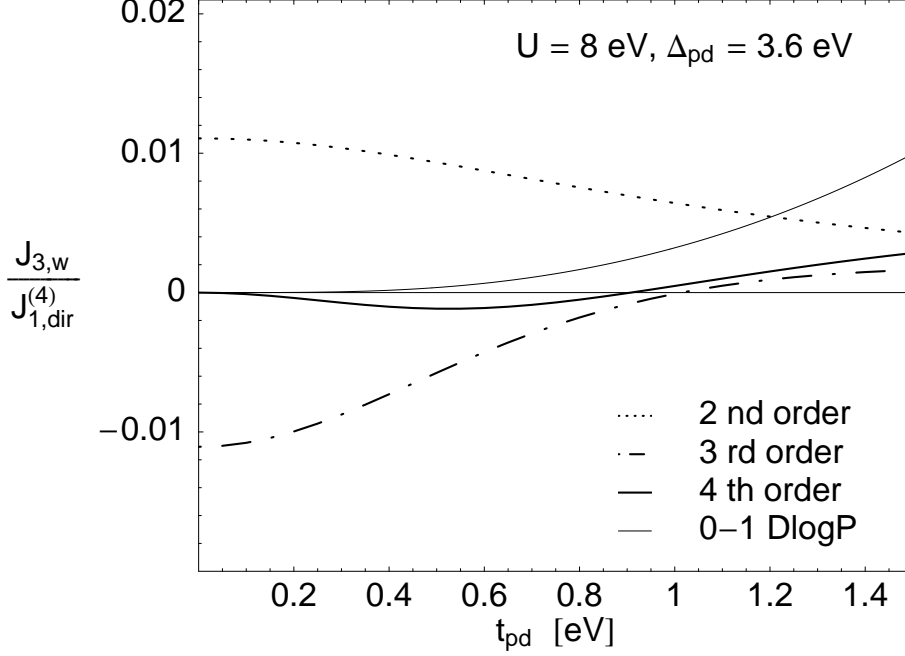


Figure 10: Variation of $J_{3,w}/J_{1,dir}^{(4)}$ with t_{pd} .

further neighbor couplings J_2 and J_3 in the Wannier representation would be very demanding. This points at definite limitations of this approach.

6 Conclusions

In the present paper we have discussed the derivation of effective spin Hamiltonians for the low energy sector of a three band model for CuO_2 -planes. By two methods we have demonstrated that it is possible to overcome the convergence problems of the t_{pd} perturbation series. Using the direct expansion with respect to t_{pd} we have derived precise values for the most important couplings via Padé approximants. The direct expansion has the advantage of a particularly simple unperturbed Hamiltonian and a very nicely localized perturbative Hamiltonian which makes high order symbolic expansions feasible. Using the Wannier representation we have confirmed the results from the direct expansion by a method with much better convergence properties. The

expansion in the Wannier representation is, however, rendered more difficult by a more complicated unperturbed Hamiltonian and a less well localized perturbative Hamiltonian and by the necessity of a non-symbolic (i.e. numerical) series expansion. Comparing the two approaches we would slightly favor the direct expansion for future applications.

The work in the present paper was confined to the most rudimentary three band model since our main goal was to demonstrate the feasibility of the derivation of accurate effective Hamiltonians. It turns out that the minimum model predicts the ratio J_{\square}/J_1 of the two important exchange couplings substantially smaller than experimental values found for cuprates. Despite of this shortcoming, we will use our results here for a demonstration fit of the couplings $J_1 = 143.3 \pm 5$ meV and $J_{\square} = 48.4 \pm 9$ meV extracted recently from the spin wave spectrum of La_2CuO_4 by Coldea et al. [11]. Assuming the typical (though somewhat arbitrary) model parameters $U = 8$ eV and $\Delta_{pd} = 3.6$ eV from (5) we obtain from the experimental value $J_1 = 143.3$ meV the estimate $1.52 \text{ eV} \leq t_{pd} \leq 1.54 \text{ eV}$ for the hopping parameter of the minimum model showing an uncertainty in t_{pd} of less than 1% due to the uncertainty of our Padé extrapolations. Assuming t_{pd} in this range our estimate for J_{\square} results in $20.8 \text{ meV} \leq J_{\square} \leq 24.8 \text{ meV}$ with an uncertainty of about $\pm 10\%$, again showing the uncertainty of our extrapolations. The estimated J_{\square} is, in fact, smaller than the experimental value by a factor of at least two.

For proper applications to cuprate materials this work will have to be extended to more realistic three band models including, in particular, a direct oxygen–oxygen hopping t_{pp} [13, 14]. The relevance of four–spin exchange has been stressed also for the two–leg ladder system $La_6Ca_8Cu_{24}O_{41}$ [27] to which the analysis presented here can be applied as well.

Acknowledgement

The authors gratefully acknowledge useful discussions with Christian Knetter and Kai Schmidt.

Appendix A

This Appendix contains the more voluminous formulae from the direct expansion of section IV. These formulae can be easily used to derive the Padé approximants discussed in section IV.

With (26) the Taylor series for the nearest neighbor exchange coupling is

$$\begin{aligned}
J_{1,\text{dir}} = & J_{1,\text{dir}}^{(4)} \left[1 - t_{pd}^2 \frac{4(7U - 2\Delta_{pd})}{(U - \Delta_{pd})^2 (2U - \Delta_{pd})} + \right. \\
& t_{pd}^4 \frac{929U^3 - 80U^2\Delta_{pd} - 60U\Delta_{pd}^2 + 12\Delta_{pd}^3}{2U^2(U - \Delta_{pd})^4 (2U - \Delta_{pd})} - \\
& t_{pd}^6 \frac{18727U^4 - 10506U^3\Delta_{pd} - 100U^2\Delta_{pd}^2 + 432U\Delta_{pd}^3 - 48\Delta_{pd}^4}{U^2(U - \Delta_{pd})^6 (2U - \Delta_{pd})^2} + \\
& t_{pd}^8 (3290060U^7 - 3541999U^6\Delta_{pd} + 1103139U^5\Delta_{pd}^2 - 139904U^4\Delta_{pd}^3 \\
& + 71509U^3\Delta_{pd}^4 - 30063U^2\Delta_{pd}^5 + 5940U\Delta_{pd}^6 - 483\Delta_{pd}^7) / \\
& \left. (4U^4(U - \Delta_{pd})^8 (2U - \Delta_{pd})^3) + O(t_{pd}^{10}) \right]. \tag{A.1}
\end{aligned}$$

The series for the four-spin coupling with the leading contribution (29) is given by

$$\begin{aligned}
J_{\square,\text{dir}} = & J_{\square,\text{dir}}^{(8)} \left[1 - t_{pd}^2 \frac{4(35U^3 - 36U^2\Delta_{pd} + 14U\Delta_{pd}^2 - 2\Delta_{pd}^3)}{(U - \Delta_{pd})^2 (2U - \Delta_{pd}) (3U^2 - 3U\Delta_{pd} + \Delta_{pd}^2)} + \right. \\
& t_{pd}^4 (460369U^7 - 699168U^6\Delta_{pd} + 305220U^5\Delta_{pd}^2 + 64524U^4\Delta_{pd}^3 \\
& - 113064U^3\Delta_{pd}^4 + 47400U^2\Delta_{pd}^5 - 9504U\Delta_{pd}^6 + 792\Delta_{pd}^7) / \\
& (40U^2(U - \Delta_{pd})^4 (2U - \Delta_{pd})^3 (3U^2 - 3U\Delta_{pd} + \Delta_{pd}^2)) \\
& - t_{pd}^6 (5381086U^8 - 9891401U^7\Delta_{pd} + 6056484U^6\Delta_{pd}^2 \\
& - 421436U^5\Delta_{pd}^3 - 1266128U^4\Delta_{pd}^4 + 715272U^3\Delta_{pd}^5 \\
& - 187864U^2\Delta_{pd}^6 + 26136U\Delta_{pd}^7 - 1584\Delta_{pd}^8) / \\
& (10U^2(U - \Delta_{pd})^6 (2U - \Delta_{pd})^4 (3U^2 - 3U\Delta_{pd} + \Delta_{pd}^2)) \\
& \left. + O(t_{pd}^8) \right]. \tag{A.2}
\end{aligned}$$

The leading contribution to the four-spin coupling (28) is

$$\begin{aligned}
J_{\times}^{(12)} = & -2t_{pd}^{12} (8511U^7 - 42784U^6\Delta_{pd} + 79536U^5\Delta_{pd}^2 - 78200U^4\Delta_{pd}^3 \\
& + 45472U^3\Delta_{pd}^4 - 15840U^2\Delta_{pd}^5 + 3072U\Delta_{pd}^6 - 256\Delta_{pd}^7) / \\
& (U^5(U - \Delta_{pd})^{11} (2U - \Delta_{pd})^2). \tag{A.3}
\end{aligned}$$

With (30) and (31) the series for the second and third neighbor two-spin couplings are given by

$$\begin{aligned}
J_{2,\text{dir}} = & J_{2,\text{dir}}^{(8)} \left[1 - \right. \\
& t_{pd}^2 \frac{4(359 U^4 - 279 U^3 \Delta_{pd} + 78 U^2 \Delta_{pd}^2 - 18 U \Delta_{pd}^3 + 2 \Delta_{pd}^4)}{(U - \Delta_{pd})^2 (2 U - \Delta_{pd}) (18 U^3 - 11 U^2 \Delta_{pd} + 5 U \Delta_{pd}^2 - \Delta_{pd}^3)} + \\
& t_{pd}^4 (365723 U^7 - 410654 U^6 \Delta_{pd} + 145422 U^5 \Delta_{pd}^2 - 22668 U^4 \Delta_{pd}^3 \\
& + 5510 U^3 \Delta_{pd}^4 - 1514 U^2 \Delta_{pd}^5 + 288 U \Delta_{pd}^6 - 24 \Delta_{pd}^7) / \\
& (4 U^2 (U - \Delta_{pd})^4 (2 U - \Delta_{pd})^2 (18 U^3 - 11 U^2 \Delta_{pd} + 5 U \Delta_{pd}^2 - \Delta_{pd}^3)) \\
& \left. + O(t_{pd}^6) \right] \quad (\text{A.4})
\end{aligned}$$

and

$$\begin{aligned}
J_{3,\text{dir}} = & J_{3,\text{dir}}^{(8)} \left[1 - \right. \\
& t_{pd}^2 \frac{2(229 U^4 - 248 U^3 \Delta_{pd} + 123 U^2 \Delta_{pd}^2 - 36 U \Delta_{pd}^3 + 4 \Delta_{pd}^4)}{(U - \Delta_{pd})^2 (2 U - \Delta_{pd}) (8 U^3 - 9 U^2 \Delta_{pd} + 5 U \Delta_{pd}^2 - \Delta_{pd}^3)} + \\
& t_{pd}^4 (325607 U^7 - 567392 U^6 \Delta_{pd} + 479098 U^5 \Delta_{pd}^2 - 278606 U^4 \Delta_{pd}^3 \\
& + 117174 U^3 \Delta_{pd}^4 - 33206 U^2 \Delta_{pd}^5 + 5712 U \Delta_{pd}^6 - 440 \Delta_{pd}^7) / \\
& (8 U^2 (U - \Delta_{pd})^4 (2 U - \Delta_{pd})^2 (8 U^3 - 9 U^2 \Delta_{pd} + 5 U \Delta_{pd}^2 - \Delta_{pd}^3)) \\
& \left. + O(t_{pd}^6) \right]. \quad (\text{A.5})
\end{aligned}$$

The 5 six-spin invariants for a hexagonal plaquette are

$$\begin{aligned}
O_1 &= (\mathbf{S}_1 \cdot \mathbf{S}_2)(\mathbf{S}_3 \cdot \mathbf{S}_4)(\mathbf{S}_5 \cdot \mathbf{S}_6) + (\mathbf{S}_2 \cdot \mathbf{S}_3)(\mathbf{S}_4 \cdot \mathbf{S}_5)(\mathbf{S}_6 \cdot \mathbf{S}_1) \\
O_2 &= (\mathbf{S}_1 \cdot \mathbf{S}_4)(\mathbf{S}_2 \cdot \mathbf{S}_6)(\mathbf{S}_3 \cdot \mathbf{S}_5) + (\mathbf{S}_2 \cdot \mathbf{S}_5)(\mathbf{S}_3 \cdot \mathbf{S}_1)(\mathbf{S}_4 \cdot \mathbf{S}_6) \\
&\quad + (\mathbf{S}_3 \cdot \mathbf{S}_6)(\mathbf{S}_4 \cdot \mathbf{S}_2)(\mathbf{S}_5 \cdot \mathbf{S}_1) \\
O_3 &= (\mathbf{S}_1 \cdot \mathbf{S}_4)(\mathbf{S}_2 \cdot \mathbf{S}_5)(\mathbf{S}_3 \cdot \mathbf{S}_6) \\
O_4 &= (\mathbf{S}_1 \cdot \mathbf{S}_2)(\mathbf{S}_3 \cdot \mathbf{S}_6)(\mathbf{S}_4 \cdot \mathbf{S}_5) + (\mathbf{S}_2 \cdot \mathbf{S}_3)(\mathbf{S}_4 \cdot \mathbf{S}_1)(\mathbf{S}_5 \cdot \mathbf{S}_6) \\
&\quad + (\mathbf{S}_3 \cdot \mathbf{S}_4)(\mathbf{S}_5 \cdot \mathbf{S}_2)(\mathbf{S}_6 \cdot \mathbf{S}_1) \\
O_5 &= (\mathbf{S}_1 \cdot \mathbf{S}_2)(\mathbf{S}_3 \cdot \mathbf{S}_5)(\mathbf{S}_4 \cdot \mathbf{S}_6) + (\mathbf{S}_2 \cdot \mathbf{S}_3)(\mathbf{S}_4 \cdot \mathbf{S}_6)(\mathbf{S}_5 \cdot \mathbf{S}_1) \\
&\quad + (\mathbf{S}_3 \cdot \mathbf{S}_4)(\mathbf{S}_5 \cdot \mathbf{S}_1)(\mathbf{S}_6 \cdot \mathbf{S}_2) + (\mathbf{S}_4 \cdot \mathbf{S}_5)(\mathbf{S}_6 \cdot \mathbf{S}_2)(\mathbf{S}_1 \cdot \mathbf{S}_3) \\
&\quad + (\mathbf{S}_5 \cdot \mathbf{S}_6)(\mathbf{S}_1 \cdot \mathbf{S}_3)(\mathbf{S}_2 \cdot \mathbf{S}_4) + (\mathbf{S}_6 \cdot \mathbf{S}_1)(\mathbf{S}_2 \cdot \mathbf{S}_4)(\mathbf{S}_3 \cdot \mathbf{S}_5). \quad (\text{A.6})
\end{aligned}$$

The leading contribution to the six-spin coupling in Eq. (32) is found to be

$$J_{\square}^{(12)} = \frac{336 t_{pd}^{12} (2U - \Delta_{pd})(26U^4 - 52U^3\Delta_{pd} + 44U^2\Delta_{pd}^2 - 18U\Delta_{pd}^3 + 3\Delta_{pd}^4)}{U^5 (U - \Delta_{pd})^{11}}. \quad (\text{A.7})$$

References

- [1] J.G. Bednorz and K.A. Müller, Z. Phys. B **64**, 189 (1986).
- [2] V.J. Emery, Phys. Rev. Lett. **58**, 2794 (1987).
- [3] Band structure calculations imply that a quantitative description of the electronic structure requires as many as eight bands, see e.g.: O.K. Andersen et al., J. Phys. Chem. Solids **56**, 1573 (1995).
- [4] F.C. Zhang and T.M. Rice, Phys. Rev. B **37**, 3759 (1988).
- [5] P.W. Anderson, Science **235**, 1196 (1987).
- [6] For a nice presentation of the method, see: M. Takahashi, J. Phys. C: Solid State Phys. **10**, 1289 (1977).
- [7] J. Stein, O. Entin-Wohlman and A. Aharony, Phys. Rev. B **53**, 775 (1996); J. Stein, Phys. Rev. B **53**, 785 (1996).
- [8] T. Yildirim et al., Phys. Rev. Lett. **73**, 2919 (1994); T. Yildirim et al., Phys. Rev. B **52**, 10239 (1995); O. Entin-Wohlman, A.B. Harris and A. Aharony, Phys. Rev. B **53**, 11661 (1996).
- [9] S. Tornow, O. Entin-Wohlman and A. Aharony, Phys. Rev. B **60**, 10206 (1999).
- [10] see also: H.J. Schmidt and Y. Kuramoto, Physica B **163**, 443 (1990); analogous results for the single band Hubbard model are obtained in [24].
- [11] R. Coldea et al., cond-mat/0006384 (2000).
- [12] For a review on the modeling of CuO_2 -planes, see: E. Dagotto, Rev. Mod. Phys. **66**, 763 (1994).

- [13] A.K. McMahan, R.M. Martin and S. Satpathy, Phys. Rev. B **38**, 6650 (1988).
- [14] M.S. Hybertsen, M. Schlüter and N.E. Christensen, Phys. Rev. B **39**, 9028 (1989).
- [15] V.J. Emery and G. Reiter, Phys. Rev. B **38**, 4547 (1988).
- [16] V.J. Emery and G. Reiter, Phys. Rev. B **38**, 11938 (1988).
- [17] F.C. Zhang and T.M. Rice, Phys. Rev. B **41**, 7243 (1990).
- [18] V.J. Emery and G. Reiter, Phys. Rev. B **41**, 7247 (1990).
- [19] H.B. Pang, T. Xiang, Z.B. Su and L. Yu, Phys. Rev. B **41**, 7209 (1990).
- [20] J. Zaanen and A.M. Oleś, Phys. Rev. B **37**, 9423 (1988).
- [21] S.V. Lovtsov and V.Y. Yushankhai, Physica C **179**, 159 (1991).
- [22] R. Hayn, V. Yushankhai and S. Lovtsov, Phys. Rev. B **47**, 5253 (1993).
- [23] A.M. Oleś, Phys. Rev. B **41**, 2562 (1990).
- [24] A.H. MacDonald, S.M. Girvin and D. Yoshioka, Phys. Rev. B **41**, 2565 (1990).
- [25] see, e.g., [20]; this paper uses the hole representation where our Δ_{pd} is replaced by $U - \Delta_{pd}$.
- [26] Products of two triple products like $[(\mathbf{S}_1 \times \mathbf{S}_2) \cdot \mathbf{S}_3][(\mathbf{S}_4 \times \mathbf{S}_5) \cdot \mathbf{S}_6]$ don't represent additional invariants since they can be expressed by scalar products.
- [27] M. Matsuda et al., J. Appl. Phys. **87**, 6271 (2000); Phys. Rev. B **62**, 8903(2000).